

# BASIC DESIGN METHODOLOGY FOR A PRILLING TOWER

Saad N. Saleh,<sup>1</sup> Shakir M. Ahmed,<sup>2</sup> Dawood Al-mosuli<sup>3</sup> and Shahzad Barghi<sup>3\*</sup>

1. Department of Chemical Engineering, University of Tikrit, Tikrit, Iraq

2. Ministry of Oil, SCOP, Iraq

3. Department of Chemical and Biochemical Engineering, Western University, London, ON, N6A 5B9, Canada

A design methodology was developed for prilling towers based on simultaneous heat, mass, and momentum balances. Basic principles of the prilling process and related sub-models were considered for production of relatively mono-size prills. The method was employed in the design of a prilling tower for production of ammonium nitrate prills from a highly concentrated solution. A special showerhead spray, operating under laminar conditions in a Rayleigh jet break-up regime, was designed to enhance production of mono-size prills. Air was used at ambient conditions. The droplets leaving the showerhead fall through the air stream in a counter-current fashion. Heat transfer from particles to air includes cooling in the fully liquid state, solidification, and cooling in the fully solid state.

The Computational Fluid Dynamics (CFD) simulation revealed the formation of a quiescent zone around the nozzle discharge region, which had a significant effect on decreasing the secondary disintegration of the droplets, and hence narrowed down the size distribution towards the desired value. The size of the produced prills was larger than the predicted value due to the formation of ammonia bubbles inside the prills.

**Keywords:** prilling tower, computational fluid dynamics (CFD), design method

## INTRODUCTION

Many solid products from chemical and other process industries, especially those produced in huge quantities, are granular, which is more convenient for use, storage, and transportation.<sup>[1]</sup> One of the major processes for granulation is to allow droplets of a salt melt or a highly concentrated solution to fall through a gaseous cooling medium and solidify into particles. These granular particles are called prills. Practically concentrated solutions of most fertilizer materials (e.g. urea and ammonium nitrate) are of low viscosity (<0.005 Pa.s) and high surface tension and can be prilled in this way.<sup>[2]</sup>

Prilling has the advantage of being able to create ideal spherical particles with a narrow size distribution and minimal external specific surface area in one single step, scalable to basically any capacity range needed.<sup>[3]</sup> The simplest method of producing uniform droplets is by discharging the molten or highly concentrated solution through an orifice nozzle, which is generally used in urea granular particle production.<sup>[4]</sup> Gezerman and Corbacioglu<sup>[5]</sup> reported that prilling tower height could affect the crystalline structure of ammonium nitrate prills. They correlated the residence time of the particle in the tower with their crystalline shape (cubic, tetragonal, and orthorhombic). Droplet size distribution can be affected by multi-frequency force disturbances in a prilling process.<sup>[6]</sup> There are two principle modes by which a liquid breaks up into droplets: liquid dripping and liquid column/jet break up mode. Various mechanisms have been proposed to account for these modes, such as the dripping mechanism, Rayleigh mechanism,<sup>[7]</sup> Weber theory,<sup>[8]</sup> and Ohnesorge criteria.<sup>[9]</sup>

The first mode occurs at low flow rates. The individual drops are formed at the tips of the nozzles. This has the advantage of giving a uniform drop size, but the output per nozzle is low, leading to a complex and expensive system. In the second mode, liquid jets are formed at higher flow rates and the breakdown of the liquid jet is caused by the growth of disturbances in the jet.<sup>[10]</sup> Generally, prills

produced with the second mode have a wide size distribution. Producing uniform droplets can be achieved by using limited types of prilling devices, such as rotating bucket or shower-type spray heads located at the top of the prilling tower. In general, the faster types of prilling devices such as the “rotating bucket” operate in the turbulent regime. The slower “showerheads” operate under laminar conditions and may have hundreds or thousands of low-capacity openings that may become filled completely and generate strings of liquid that break up into droplets. The droplet size is closely linked to the actual size of the openings.<sup>[3]</sup>

Procedures for designing a prilling tower depend on the individual, based on practical experience, together with laboratory-scale tests and basic principles. By using data on melting point, viscosity, surface tension, etc., of the material, together with laboratory-scale tests, it is possible to specify optimum temperature, pressure, orifice size, and gas flow conditions for the required prill size and quality.<sup>[11]</sup> Honti<sup>[12]</sup> used solidifying time as the key parameter in determining the height of a prilling tower.

Prills may be also produced using a rotating perforated cylindrical drum, which contains molten liquid. As a result of drum rotation, curved liquid jets emanating from the perforations break up into droplets due to centrifugal and gravitational forces.<sup>[13]</sup> Aadil et al.<sup>[14]</sup> studied the formation of droplets from breakup of a liquid jet formed through a perforated rotating bucket and showed that liquid exit velocity and viscosity were dominant parameters for prediction of droplet size distribution. CFD was successfully employed in the study of internal flow field for the

\* Author to whom correspondence may be addressed.

E-mail address: sbarghi2@eng.uwo.ca

Can. J. Chem. Eng. 93:1403–1409, 2015

© 2015 Canadian Society for Chemical Engineering

DOI 10.1002/cjce.22230

Published online 4 June 2015 in Wiley Online Library

(wileyonlinelibrary.com).

prilling applications in a perforated rotating bucket. It was shown that the velocity field in the bucket had great effects on heat and mass transfer in the prilling process.<sup>[15]</sup> A more in-depth study to investigate the trajectory and stability of a spiraling inviscid liquid jet from a rapidly rotating orifice resulted in a determination of the jet breakup length.<sup>[16]</sup>

The objective of the present work is to develop a design methodology for prilling towers by combining fundamental principles of fluid mechanics and transport phenomena. The criteria for production of relatively mono-size prills are investigated. The design equations contain all the required parameters and provide an easy platform to investigate the effects of such parameters on the design and operation of the prilling tower. The flow pattern of cooling air inside the prilling tower is also investigated. CFD is employed to verify the design and gas flow pattern inside the tower. The results are compared with data from a commercial plant using a prilling tower for production of ammonium nitrate.

## DESIGN METHODOLOGY

The theoretical basis of a process consisting of spraying the feed, droplet size distribution, droplet solidification while cooling by air, and additional cooling in the fully solid state is reviewed in detail. Governing equations for each stage are presented, followed by the determination of prilling tower size. Finally, CFD modelling is employed to verify the design results.

### Spraying

In the prilling process, the operation of spraying devices may range from very fast, highly turbulent, and disordered to slow, laminar, and ordered conditions.

Based on the pioneering works of Rayleigh and Weber,<sup>[7,8]</sup> producing very uniform droplets is generally limited to a showerhead spray type, which operates under laminar conditions. For steady injection of a liquid through a single nozzle with circular orifices into a quiescent gas, the mechanisms of jet breakup are typically classified into four primary regimes influenced by inertial, surface tension, viscous, and aerodynamic forces. These regimes are Rayleigh, first wind induced, second wind induced, and atomization regimes. A detailed review of these regimes can be found elsewhere.<sup>[17-21]</sup>

Mono-dispersed particles can be produced by operating the showerhead in the Rayleigh jet breakup regime, considering the following criteria for Rayleigh jet breakup:<sup>[22]</sup>

$$We_l > 8 \quad \text{and} \quad We_g < 0.4 \quad \text{or} \quad 1.2 + 3.41Oh^{0.9} \quad (1)$$

where

$$We_l = \frac{\rho_l d u_l^2}{\sigma}, \quad We_g = \frac{\rho_g d (u_l - v_g)^2}{\sigma}, \quad Oh = \frac{\mu_l}{\sqrt{\rho_l \cdot d \cdot \sigma}}$$

The Weber number ( $We$ ) is a measure of the ratio between drag force and surface tension effects,  $\mu$  is the viscosity,  $\rho$  is the density,  $\sigma$  is surface tension,  $u$  and  $v$  are liquid and gas velocities respectively, and  $d$  is the nozzle diameter. The Ohnesorge number ( $Oh$ ) describes the ratio between viscous effects and surface tension in the liquid.

To operate the showerhead in the Rayleigh jet breakup regime, the internal flow of the circular orifice nozzle must be in a single phase state, where the liquid completely fills the orifice as shown in Figure 1.<sup>[23]</sup>

The mass flow rate of the nozzle is defined by:

$$M = C_d A \sqrt{2\rho(p_1 - p_2)} \quad (2)$$

where the discharge coefficient  $C_d$  is:<sup>[24]</sup>

$$C_d = \frac{1}{\frac{1}{C_{dU}} + 20 \frac{(1+2.25L/d)}{Re_h}} \quad (3)$$

where  $C_{dU}$  is the ultimate discharge coefficient and is defined as:

$$C_{dU} = 0.827 - 0.0085 \frac{L}{d} \quad (4)$$

Generally  $C_d$  is around 0.62.

The Reynolds number based on hydraulic head ( $Re_h$ ) is:

$$Re_h = \frac{d\rho_l}{\mu} \sqrt{\frac{2(p_1 - p_2)}{\rho_l}} \quad (5)$$

For a single-phase nozzle, calculation of the exit velocity comes from the conservation of mass and the assumption of a uniform exit velocity as  $u_l = M/(\rho_l A)$ .

Finally, the Rayleigh-Weber equation<sup>[18]</sup> is used to calculate the droplet diameter.

$$\lambda_{opt} = \sqrt{2\pi} d \left( 1 + \frac{3\mu_l}{\sqrt{\rho_l \sigma d}} \right)^{0.5} \quad (6)$$

$$D = (1.5 \lambda_{opt} d^2)^{1/3} \quad (7)$$

where  $\lambda_{opt}$  is the wavelength of the liquid column at the optimum perturbation.

### Droplet Solidification

The molten droplets leave the plain orifice (shower heads) only slightly above their melting point  $T_m$ . The droplets of radius  $R$  are

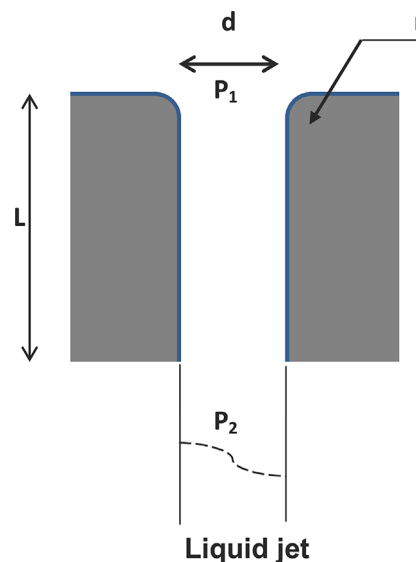


Figure 1. Single phase nozzle flow.<sup>[23]</sup>

solidified at  $T_m$  and cooled to  $T_{p1}$  as they fall through a counter-current stream of air at  $T_a$ . Both the heat of solidification and the sensible heat must be removed, and in many instances solid phase transition must be allowed for.

For the purpose of analysis, the thermal history of a falling droplet can be divided into three regions.

#### Cooling in fully liquid state

Assuming a spherical droplet, the change in internal heat content due to convective heat transfer can be expressed by:

$$c_{p,l} \frac{dT_p}{dt} = -\frac{6h}{\rho_p D_p} (T_p - T_a) \quad (8)$$

where  $h$  is the overall heat transfer coefficient. The Ranz-Marshall correlation<sup>[25]</sup> has frequently been used to determine the heat transfer coefficient:

$$h = \frac{k_a}{D} (2 + 0.6\text{Re}^{0.5}\text{Pr}^{0.33}) \quad (9)$$

In Equation 9, the air turbulence effect during heat transfer from the droplets is assumed to be negligible.

#### Solidification

The solidification stage can be described by the time-dependent heat conduction equation in spherical coordinates:

$$\frac{\partial T}{\partial t} = \frac{k}{\rho C_p} \frac{1}{r^2} \frac{\partial}{\partial r} \left( r^2 \frac{\partial T}{\partial r} \right) \quad (10)$$

using the following boundary conditions:

$$\frac{\partial T}{\partial r} = 0 \quad r = 0 \quad t > 0 \quad (11)$$

$$-k \frac{dT}{dr} = h(T - T_a) \quad r = R \quad t > 0 \quad (12)$$

$$T = T_m \quad t = 0 \quad 0 < r < R \quad (13)$$

Since the droplets sprayed by the shower heads are considered coarse material, the rate at which the centre of the droplet reaches a specified temperature is controlled by internal conduction. The first boundary condition arises from symmetry considerations. The second boundary condition describes the case of heat lost from the droplet to the surrounding air according to Newton's law of cooling, with a constant heat transfer coefficient ( $h$ ), with the final boundary condition prescribing an initially uniform temperature profile within the droplet.

Special consideration is required for handling this model because the inner boundary condition (at  $t > 0$ ,  $T = T_m$  and  $r = R_s$ ) moves relative to the centre of the droplet during the process.

The analytical solution for this case is obtained by equating the heat liberation at  $r = R_s(t)$  (the liquid-solid interface) resulting from the solidifying of the droplet to the heat flow across the spherical surface at  $r = R$  (the solid-air interface).

$$t_s = \frac{\rho \Delta H_s R}{h(T_m - T_a)} \left[ \frac{1}{3} + \frac{1}{6} \frac{hR}{k} \right] \quad (14)$$

where  $\Delta H_s$  is the latent heat of solidification.

#### Cooling in the fully solid state

After the droplet is completely solidified, it cools further in the solid state. Similar to Equation (8), this process can be evaluated from:

$$c_{p,s} \frac{dT_p}{dt} = -\frac{6h}{\rho_p D_p} (T_p - T_a) \quad (15)$$

Within a typical spray-forming application and relatively low to moderate temperatures, the heat transfer due to convection is almost two orders of magnitude higher than the heat transfer due to radiation. Therefore the heat transfer due to radiation from the droplet is neglected.<sup>[19]</sup>

#### Sizing the Tower

Prilling is a dynamic process where jets of concentrated/molten liquid are formed at the showerhead and broken into droplets. The droplets fall down while they are solidified and cooled by heat transfer to a counter-current air stream. The droplets start to fall with a finite velocity and accelerate or decelerate to their terminal velocities.

The motion of particles in the air flow field is described in a Lagrangian way by solving a set of ordinary differential equations along the trajectory in order to calculate the change of particle location and the components of the particle velocity. This requires the consideration of all relevant forces acting on the particle. Inter-particle forces, such as van der Waals forces, capillary forces, and electrostatic forces are neglected since the particles used in this study are large and inter-particle forces are insignificant compared to gravity, buoyant, and drag forces.

The equation of motion can be derived from balancing the forces acting on the droplet using Newton's second law of motion.<sup>[26]</sup>

$$m_p \frac{d\vec{u}}{dt} = \frac{C_D \rho_a A_p |\vec{v} - \vec{u}| (\vec{v} - \vec{u})}{2} + \frac{\pi}{6} D^3 (\rho_p - \rho_a) \vec{g} - \frac{\pi}{4} D^3 \rho_a \Delta P \quad (16)$$

The first term denotes the drag force and the second term is the buoyant force, and since the particle density is much larger than the air density, this term constitutes the gravitational force. The last term is the pressure gradient force and is negligible in the prilling process. Therefore, the equation of motion for a droplet is simplified to:

$$m_p \frac{d\vec{u}}{dt} = \frac{C_D \rho_a A_p |\vec{v} - \vec{u}| (\vec{v} - \vec{u})}{2} + m_p \vec{g} \quad (17)$$

From the dependence of the drag coefficient of a spherical particle on the Reynolds number, one may identify several regimes (Stokes, transition, and Newton) associated with the flow characteristics around the sphere.<sup>[27,28]</sup>

A frequently-used correlation for the drag coefficient is (Schiller & Naumann<sup>[29]</sup>):

$$C_D = \frac{24}{\text{Re}_p} (1 + 0.15 \text{Re}_p^{0.687}) \quad (18)$$

where  $\text{Re}_p$  denotes the particle Reynolds number:

$$\text{Re}_p = \frac{\rho_a D_p |\vec{v} - \vec{u}|}{\mu_a} \quad (19)$$

The particle terminal velocity can be estimated assuming one-dimensional flow for both particles and air in a vertical direction inside the prilling tower.<sup>[11]</sup> Terminal velocity conditions occur when the buoyant force and drag force are balanced by gravity.<sup>[30]</sup>

$$\frac{\pi}{6}D^3(\rho_p - \rho_a)\vec{g} = \frac{C_D\rho_a A_p |\vec{v} - \vec{u}|(\vec{v} - \vec{u})}{2} \quad (20)$$

$$u_v - v = \sqrt{\frac{4D(\rho_p - \rho_a)g}{3C_D\rho_a}} \quad (21)$$

In the case of prilling, Equation (18) can be used to replace  $C_D$ .

In order to complete the analysis of the particle's motion, the distance-time relationship can be obtained by rearranging Equation (17):

$$\frac{d(u_v - v)}{dt} = \frac{g(\rho_p - \rho_a)}{\rho_p} - \frac{C_D\rho_a A_p |u_v - v|(u_v - v)}{2m_p} \quad (22)$$

where

$$m_p = \frac{1}{6}\pi D^3 \rho_p, \quad A_p = \frac{1}{4}\pi D^2$$

Equation (22) is identical to the Lapple and Shepherd equation<sup>[31]</sup> in calculating particle trajectories from a nozzle or atomizer in non-rotating air, where the movement in the vertical direction is more dominant.

Therefore, the effective height of the tower is determined as the vertical distance that a droplet of average size ( $D_{50}$ ) travels from the showerhead to the base of the tower during the estimated time for solidifying and cooling to the desired temperature.

The diameter of the prilling tower is determined primarily by the number of spray nozzles necessary for the desired production rate, where the prilling tower must have sufficient space to envelope the flight paths of the biggest droplets ( $D_{99}$ ). The biggest particles must not hit the wall before they are sufficiently solidified. The sizes of the biggest prills was estimated using Kjaergaard's model<sup>[7]</sup> where:

$$D_{99} = 1.5D_{50} \quad (23)$$

The critical time of flight for the biggest droplets ( $D_{99}$ ) is when the outer 1/3 of the mass of droplet has solidified. At this stage, contact with the walls is considered safe (no disintegration).<sup>[7]</sup>

#### CFD Modelling

CFD simulation can be applied to examine prilling tower design. It predicts the air flow and calculates the trajectories of the prills, and then determines the hitting regions of the walls. Using CFD Fluent 6.3, the air phase is modelled as continuum using the Euler approach and the droplet/particle phase is modelled by the Discrete Phase model (Lagrange approach).<sup>[23]</sup> In essence, CFD is a numerical solution of the equations governing fluid flow in the prilling tower; this involves generating a mesh that divides the flow region of interest into a large number of small control volumes.<sup>[32]</sup> Simple algebraic equations can then be developed for each control volume to describe the conservation of mass, momentum, and energy.

#### CASE STUDY

The design data from the AL-Hadar establishment for the production of fertilizers in Ninawa state in Iraq for the production of high density ammonium nitrate (20 ton/day) was used in this study. The concentrated (99.8 %) ammonium nitrate solution was fed at 180 °C to the prilling device (shower-type spray head) located at the top of the prilling tower as shown in Figure 2. The liquid droplets fell from the shower head counter-currently through an air stream entering the tower at ambient temperature (about 25 °C). Air was sucked into the base of the tower by exhaust fans mounted on top of the tower. The product was removed from the tower base to a conveyor belt using a conical hopper.

#### RESULTS AND DISCUSSION

For the purposes of illustration, the results of the design calculations are summarized in Table 1 at the operating conditions of the case described above. Eight showerheads fabricated in the plant workshop were installed at the top of the tower for spraying highly concentrated ammonium nitrate solution (0.998 g/g, 99.8 wt%). Each showerhead contains forty holes distributed in concentric circles. The number in use is adjusted to fit the rate of operation. Figure 3 shows the arrangement of spray heads at the top of the tower.

The diameter and effective height of the tower provides a flight time for the biggest droplets ( $D_{99}$ ) of 4.5 s, which is predicted by the CFD simulation. This flight time is greater than the time needed to solidify 1/3 of the mass of the biggest droplets, which is calculated using Equation (14).

The produced particles have a relatively uniform measured size of 2.3 mm and are spherical or spheroidal in shape, which is different from the predicted size of 1.92 mm, most likely due to the

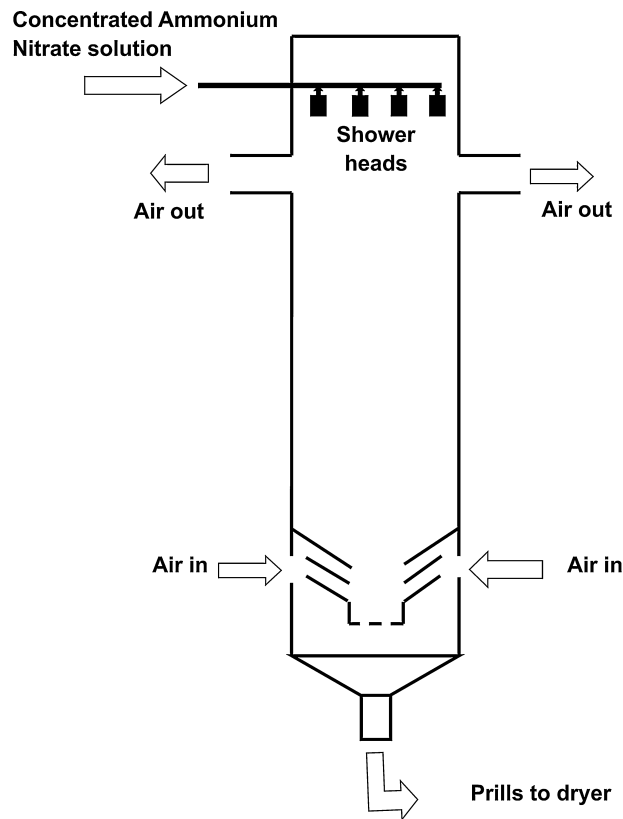


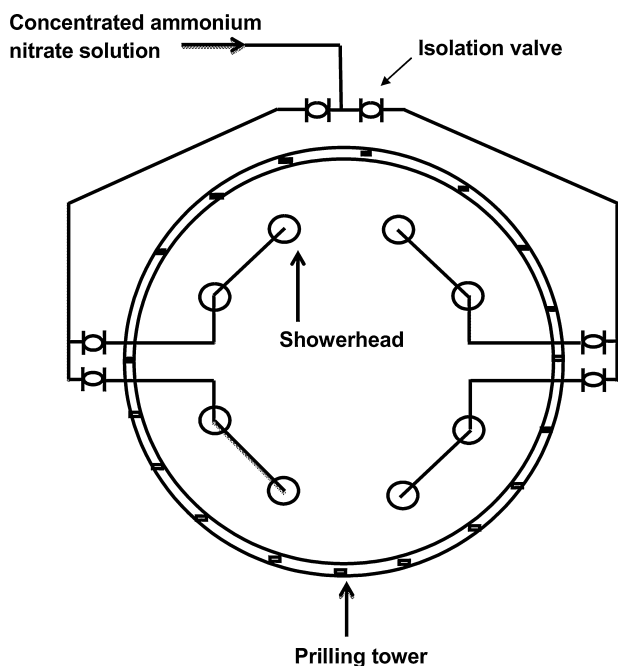
Figure 2. Prilling process of ammonium nitrate solution.

**Table 1.** Results of design calculations

Effective height of tower, m	30.00
Diameter of tower, m	2.80
Nozzle diameter, mm	1.00
Nozzle length, mm	5.00
No. of exhaust fans	4.00
Average particle size, mm	1.92
Biggest particle size, mm	2.90
Air flow rate, m <sup>3</sup> /s	6.11
Air velocity, m/s	1.00
No. of showerhead	8.00

way the generic morphology of the final prills is attained. In industry, all the stages of the operations during the manufacturing of ammonium nitrate take place in excess of ammonia, where the alkaline medium delays thermal decomposition and improves the quality of the product.<sup>[33]</sup> Ammonia is liberated during solidification of the droplets resulting in an inflation of the prills.<sup>[34]</sup> This explains why the size of the produced prills in industry is different from the size of pure ammonium nitrate prills.

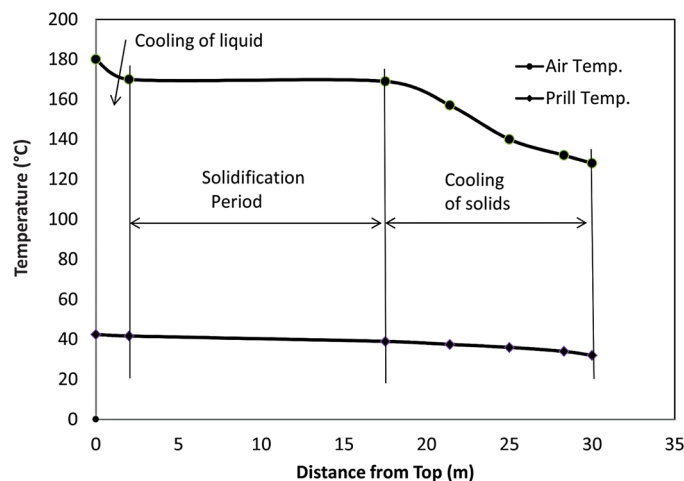
It was noted that the particles of sizes < 1 mm comprised less than 5 % of the mass of product, which was collected at the bottom of the prilling tower. This firstly indicated that secondary disintegration rarely took place when using the showerheads for spraying in comparison with other types of atomization devices. Secondly, the selection of the spraying temperature was correct (180 °C) where a higher temperature would cause the rapid release of ammonia, which results in an efflorescence of the prills, and this has a significant effect on the performance of the prilling process. The efflorescence reveals that effluents in the form of prills carry over, which are sucked through air exhaust fans to the atmosphere. In addition to a loss of production capacity, this causes air pollution. Therefore, the contamination may be minimized by careful design of prilling devices, the selection of spraying temperature, and optimization

**Figure 3.** Arrangement of spray heads at the top of the prilling tower.

of the average velocity of air through the tower, where higher air velocity results in the escape of larger particles. Thus the mass of particles carried over increases very rapidly with air velocity. In this design, the average velocity of air through the tower was 1.0 m/s.

As depicted in Figure 4, the prill temperature profile shows three distinct stages: a) the first stage of rapid cooling in the vicinity of the showerhead due to high temperature of highly concentrated prills, which results in high heat transfer to the exit air; b) the second stage with a relatively constant temperature profile, which is associated with the solidification process where latent heat of melting leaves the prills at a relatively constant temperature; c) the third stage of cooling, where the solidified prills are cooled by contacting the incoming air to the tower. The air temperature increases due to the heat transfer from the prills. For the specific operating conditions in this study, the air temperature does not change significantly; however different temperature profiles may be obtained if air flow rate and temperature change.

One of the main challenges in operation of the prilling tower is blockage of the orifices of the showerheads at discrete periods due to the presence of impurities. The impurities may be due to oxidation of the pipes and equipment or other contaminants in the concentrated liquid feed. These suspended impurities may build up inside the orifice holes. To avoid this specific problem, it is suggested to install a vibrated system that helps to avoid buildup of solid materials in the holes. An additional advantage of the vibrated system is that it leads to a continuous breakup of the liquid jet into approximately identical droplets. In several applications, prills of almost identical size are needed, therefore in operation of the prilling process, it is necessary to obtain substantially mono-dispersed droplets by operating the showerheads in the Rayleigh jet breakup regime. In order to operate in the Rayleigh jet breakup regime, the liquid must attain a certain velocity at the showerhead, which can be achieved by increasing the hydrostatic pressure on the shower heads or using a properly designed pump. The air velocity also plays an important role in attaining this regime, by creating a relatively quiescent zone near the showerheads. In the quiescent zone, the air friction decreases, the optimum wavelength increases, and consequently the droplet diameter increases. This quiescent zone was 1.7 m distant from the showerheads to the air outlet as shown in Figure 2. This zone is very clear in the predicted contour of air

**Figure 4.** Temperature profile for air and prills (1.92 mm in size) inside the prilling tower.

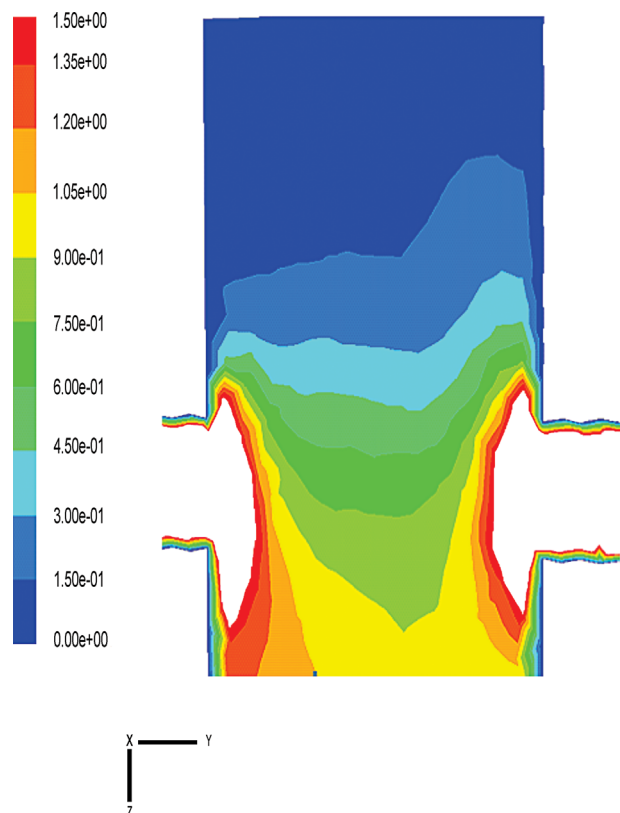


**Figure 5.** Contour of predicted air velocity (m/s) in the upper section of the prilling tower.

velocity (Figure 5) by the CFD simulation, where the predicted air velocity in this zone is approximately 0.1 m/s.

## CONCLUSIONS

A design method was developed for the prilling process. Design equations and related sub-models were properly integrated into a rigorous design method, which was backed up by a CFD simulation. In order to achieve mono-dispersing prills and reduce prill carryover, a spray-type showerhead was selected to obtain relatively mono-dispersed droplets due to the creation of a relatively quiescent zone near the showerheads. Formation of a quiescent zone led to reduction in air velocity and friction and increased wavelength, resulting in the production of larger mono-size prills.

Regarding the production of industrial ammonium nitrate, the average particle size was larger than pure ammonium nitrate due to the inflation of particles caused by formation of ammonia bubbles located inside the particles. Therefore, in addition to spraying ability, the physical-chemical properties of the material must be carefully considered before proceeding with the tower design.

## NOMENCLATURE

$A$	cross-sectional area (m <sup>2</sup> )
$A_p$	projected area of particle (m <sup>2</sup> )
$C_D$	drag coefficient
$C_d$	discharge coefficient
$C_{dU}$	ultimate discharge coefficient
$C_p$	specific heat (kJ/kg.K)

$d$	nozzle diameter (mm)
$D_p$	particle diameter (mm)
$D_{50}$	average particle size (mm)
$D_{99}$	biggest particle size (mm)
$g$	gravitational acceleration (m/s <sup>2</sup> )
$h$	heat transfer coefficient (kW/m <sup>2</sup> .K)
$\Delta H_s$	solidification heat (kJ/kg)
$K$	cavitation number
$k$	thermal conductivity (kW/m.K)
$L$	nozzle length (mm)
$m$	droplet mass (kg)
$M$	mass flow rate through the nozzle (kg/s)
$Oh$	Ohnesorge number
$P$	pressure (Pa)
$Pr$	Prandtl number
$R$	radius (mm)
$r$	radius of nozzle curvature and radial coordinate (mm)
$T$	temperature (K)
$t$	time (s)
$Re$	Reynolds number
$Sc$	Schmidt number
$Sh$	Sherwood number
$u$	velocity (m/s)
$v$	velocity (m/s)
$We$	Weber number

## Greek Letters

$\lambda$	wavelength (mm)
$\mu$	viscosity (kg/m.s)
$\rho$	density (kg/m <sup>3</sup> )
$\sigma$	surface tension (N/m)

## Subscripts

$a$	air
$crit$	critical
$d$	droplet
$eff$	effective
$g$	gas
$h$	hydraulic head
$incept$	inspection
$l$	liquid
$m$	melting
$opt$	optimum
$p$	droplet/particle
$s$	solid
$V$	vapour
$v$	vertical
$1$	upstream
$2$	downstream

## REFERENCES

- [1] W. Yaun, B. Chuanping, Z. Yuxin, *Chin. J. Chem. Eng.* **2007**, *15*, 424.
- [2] F. E. Steenwinkel, J. W. Hoogendonk, "The Prilling of Compound Fertilizers," *Proceedings of the International Fertiliser Society*, Colchester, UK **1969**, p. 109.
- [3] O. G. Kjaergaard, "Prilling-multiple core encapsulation," *GEA-Niro A/S R1 Aug.* **2000**, accessed on 26 January 2014,

- [http://www.niroinc.com/food\\_chemical/prilling\\_encapsulation.asp](http://www.niroinc.com/food_chemical/prilling_encapsulation.asp).
- [4] N. Rahmanian, M. Homayoonfard, A. Alamdari, *Chem. Eng. Commun.* **2013**, *20*, 764.
- [5] A. O. Gezerman, B. D. Corbacioglu, *Int. J. Chem.* **2011**, *3*, 158.
- [6] C. J. Gurney, M. J. H. Simmons, V. L. Hawkins, S. P. Decent, *Chem. Eng. Sci.* **2010**, *65*, 3474.
- [7] L. Rayleigh, *Proc. Lond. Math. Soc.* **1878**, *10*, 4.
- [8] G. Weber, *Z. Angew. Math. Mech.* **1931**, *11*, 136.
- [9] W. V. Ohnesorge, *Z. Angew. Math. Mech.* **1936**, *16*, 355.
- [10] A. G. Roberts, K. D. Shah, *The Chemical Engineer* **1975**, *Dec.*, 748.
- [11] R. H. Perry, D. W. Green, *Perry's chemical engineers' handbook*, 6<sup>th</sup> edition, McGraw Hill, New York **1984**.
- [12] G. D. Honti, *The nitrogen industry*, 15<sup>th</sup> edition, Akadémiai Kiadó, Budapest **1976**.
- [13] J. Uddin, S. P. Decent, M. J. H. Simmons, *Int. J. Eng. Sci.* **2008**, *46*, 1253.
- [14] A. Muhammad, N. Rahmanian, R. Pendyala, *J. Appl. Sci.* **2014**, *14*, 1252.
- [15] A. Muhammad, N. Rahmanian, R. Pendyala, *Appl. Mech. Mater.* **2013**, *372*, 340.
- [16] I. M. Wallwork, S. P. Decent, A. C. King, R. M. S. M. Schulkes, *J. Fluid Mech.* **2002**, *459*, 43.
- [17] C. T. Crowe, *Multiphase flow handbook*, Taylor and Francis Group, Abingdon, UK **2006**.
- [18] H. Liu, *Science and engineering of droplets fundamental and applications*, Noyes Publications, New York **2000**.
- [19] U. Fritsching, *Spray simulation*, Cambridge University Press, New York **2004**.
- [20] C. Dumouchel, *Exp. Fluids* **2008**, *45*, 371.
- [21] S. P. Lin, R. D. Rietz, *Annu. Rev. Fluid Mech.* **1998**, *30*, 85.
- [22] C. Soteriou, R. M. Andrews, M. Smith, "Direct Injection Diesel Sprays and the Effect of cavitation and Hydraulic Flip on Atomization," SAE Paper 950080, SAE, Warrendale, PA, USA **1995**.
- [23] ANSYS Fluent, "Fluent Theory Guide," Chap. 15: Discrete phase, Release 14 **2011**.
- [24] A. K. Lichtarowicz, R. K. Duggins, E. Markland, *J. Mech. Eng. Sci.* **1965**, *7*, 2.
- [25] W. E. Ranz, W. R. Marshall, *Chem. Eng. Prog.* **1952**, *48*, 173.
- [26] M. H. Askel, O. C. Erlap, *Gas Dynamics*, Prentice Hall, UK **1994**.
- [27] M. Sommerfeld, "Theoretical and experimental modeling of particulate flows," *von Karman institute for fluid dynamics* **2000**, accessed 26 January 2014, [http://lvov.weizmann.ac.il/Literature-Online/Literature/Lectures/2000\\_Modelling\\_-\\_Particulate\\_Flows.pdf](http://lvov.weizmann.ac.il/Literature-Online/Literature/Lectures/2000_Modelling_-_Particulate_Flows.pdf)
- [28] G. G. Stokes, *Cambr. Phil. Soc.* **1851**, *9*, 8.
- [29] L. Schiller, A. Naumann, *Ver. Deut. Ing.* **1933**, *44*, 318.
- [30] K. Masters, *Spray Drying Handbook*, 4th edition, John Wiley & Sons, New York **1985**.
- [31] C. E. Lapple, C. B. Shepherd, *Ind. Eng. Chem.* **1940**, *23*, 605.
- [32] H. K. Versteeg, W. Malalasekera, *An introduction to computational fluid dynamics-the finite volume method*, Longman Group Ltd., Harlow, UK **1995**.
- [33] W. H. Shearon, W. B. Dunwoody, *Ind. Eng. Chem.* **1953**, *45*, 496.
- [34] Z. Krawiec, "Physico-chemical properties of the ammonium nitrate-ammonia system and their relation to aerosol and dust emission in ammonium nitrate prilling process," *IFA Technical Conference* **1992**, accessed 26 January 2014, <http://eurekamag.com/research/002/457/002457552.php>

---

*Manuscript received June 3, 2014; revised manuscript received September 26, 2014; accepted for publication October 7, 2014.*